Angle-Based Codebook for Low-Resolution Hybrid Precoding in Millimeter-Wave Massive MIMO Systems

(Invited Paper)

Jingbo Tan*, Linglong Dai*, Jianjun Li†, and Shi Jin‡
*Tsinghua National Laboratory for Information Science and Technology (TNList)
Department of Electronic Engineering, Tsinghua University, Beijing 100084, P. R. China
†The School of Electric and Information Engineering, Zhongyuan University of Technology, Zhengzhou 450007, P. R. China
‡National Mobile Communications Research Laboratory, Southeast University, Nanjing 210096, P. R. China
E-mail: tanjb13@mails.tsinghua.edu.cn

***Abstract*—Hybrid precoding is a promising technique for millimeter-wave massive MIMO systems, as it can significantly reduce the number of radio-frequency (RF) chains with near-optimal performance. To further reduce the power consumption, low-resolution hybrid precoding utilizing low-resolution phase shifters is recently proposed without an obvious performance loss. However, traditional channel feedback codebooks that quantize the channel with high resolution are not suitable to low-resolution hybrid precoding. In this paper, we design an angle-based codebook for low-resolution hybrid precoding, where the analog codebook is designed based on channel angle-of-departures (AoDs), while the digital codebook is designed by random vector quantization (RVQ). As the angle coherence time is much longer than the channel coherence time, the selected analog codeword from the analog codebook remains unchanged in a much longer time scale. Thus, the channel feedback overhead can be significantly reduced. Simulation results illustrate that the proposed codebook with low overhead for channel feedback is able to achieve the acceptable sum-rate performance.**

I. Introduction

Due to the wider bandwidth and higher frequency efficiency, millimeter-wave (mmWave) massive multiple-input multiple-output (MIMO) has been considered to be one of the promising techniques for future 5G wireless communications [1], [2]. In mmWave massive MIMO systems, the classical fully digital precoding will cause unaffordable hardware complexity and power consumption, where the required number of radio-frequency (RF) chains is equal to the large antenna number. To solve this challenging problem, hybrid precoding has been recently proposed to significantly reduce the number of RF chains [3]–[7]. The key idea of hybrid precoding is to decompose the large-size fully digital precoder into a large-size analog precoder and a small-size digital precoder. Due to the sparse characteraitics of mmWave channels, it has been proved that hybrid precoding is able to achieve the near-optimal sum-rate performance [8].

Accurate channel state at the transmitter (CSIT) is essential to achieve the near-optimal sum-rate performance of hybrid precoding [9]–[12]. Various channel feedback schemes have been proposed to realize accurate CSIT. Specifically, a two-stage hybrid precoding scheme with limited feedback was proposed in [13], where the beamsteering codebook and random vector quantization (RVQ) codebook are used for analog and digital precoder, respectively. In [14], a codebook that linearly combines traditional discrete fourier transform (DFT) codewords was designed to quantize the channel more accurately for channel feedback. In addition, a hierarchical codebook was proposed [15] to form the analog precoder for hybrid precoding via the multi-RF-chain sub-array technique. However, all of these existing channel feedback schemes only consider high-resolution phase shifters (e.g., 8 bits), which may cause large energy consumption when a large number of PSs are used for hybrid precoding [16]. The recently proposed low-resolution hybrid precoding using low-resolution PSs (e.g., 1-2 bits) is attractive due to its higher energy efficiency and acceptable sum-rate performance [6], [17]. In [6], a machine learning based low-resolution hybrid precoding method was proposed. In [17], the near-optimal low-resolution hybrid precoder was designed by projecting the optimal precoder to the subspace decided by low-resolution PSs constraint. However, these methods are proposed under the accurate CSIT assumption. On the other hand, for low-resolution hybrid precoding, the existing channel feedback schemes, which quantize the channel with high resolution, are not suitable for low-resolution PSs. Therefore, it is important to design a codebook suitable for low-resolution hybrid precoding, which has not been investigated in the literature to the best of our knowledge.

To fill in this gap, we design an angle-based codebook for low-resolution hybrid precoding in this paper[1]. Specifically, the high-dimensional analog codebook is designed based on channel angle-of-departures (AoDs) through a neighbor search algorithm, while the traditional RVQ codebook is applied for low-dimensional digital precoder. Under the framework of angle coherence time [18], the analog codewords selected from the proposed angle-based codebook remains unchanged for a much longer time than the channel coherence time, which significantly reduces the channel feedback overhead. Simulation results verify that the proposed angle-based codebook is

[1]The simulation codes are provided to reproduce the results in this paper at http://oa.ee.tsinghua.edu.cn/dailinglong/publications/publications.html.

978-1-5386-4502-4/17/$31.00 ©2017 IEEE

able to achieve the acceptable sum-rate performance with low overhead for channel feedback.

Notation: Lower-case and upper-case boldface letters denote vectors and matrices, respectively; $(\cdot)^T$, $(\cdot)^H$, and $\|\cdot\|_F$ denote the transpose, conjugate transpose, and Frobenius norm of a matrix, respectively; $|\cdot|$ denotes the absolute operator; $\mathbb{E}(\cdot)$ denotes the expectation; I_N is the $N \times N$ identity matrix; $\binom{n}{k}$ is the number of k-combinations of a set of size n.

II. System Model

In this section, the mmWave channel model is briefly described at first. Then, we introduce the low-resolution hybrid precoding, and the array gain performance of this architecture will be analyzed in the end.

A. Channel Model

In this paper, we consider a typical mmWave massive MIMO system with hybrid precoding. The base station (BS) employs the widely used uniform linear array (ULA) of M antennas and M_{RF} RF chains, where $M_{\mathrm{RF}} \ll M$ for hybrid precoding. The $N \times 1$ received signal vector $\mathbf{y}$ at the user with N antennas can be represented as

$$\mathbf{y} = \mathbf{H}\mathbf{F}_{\mathrm{RF}}\mathbf{F}_{\mathrm{BB}}\mathbf{s} + \mathbf{n}, \tag{1}$$

where $\mathbf{H} = [\mathbf{h}_1, \mathbf{h}_2, \cdots, \mathbf{h}_N]^T$ of size $N \times M$ is the channel matrix in which $\mathbf{h}_n$ denote the $M \times 1$ channel vector between the M-antenna BS and the n-th antenna of the user, $\mathbf{F}_{\mathrm{RF}}$ of size $M \times M_{\mathrm{RF}}$ is the analog precoder realized by P-bit PSs whose elements belong to $\frac{1}{\sqrt{M}}\{1, e^{j\frac{1}{2^P-1}\pi}, \cdots, e^{j\frac{2^P-1}{2^P-1}\pi}\}$, $\mathbf{F}_{\mathrm{BB}}$ of size $M_{\mathrm{RF}} \times N$ is the baseband digital precoder with the total transmit power constraint $\|\mathbf{F}_{\mathrm{RF}}\mathbf{F}_{\mathrm{BB}}\|_F^2 = \rho$, $\mathbf{s}$ is the $N \times 1$ transmitted signal vector satisfying $\mathbb{E}(\mathbf{s}\mathbf{s}^H) = \mathbf{I}_N$. Finally, the additive white Gaussian noise (AWGN) vector $\mathbf{n} \sim \mathcal{CN}(0, \sigma^2\mathbf{I}_N)$, where σ^2 presents the noise power.

For the channel matrix $\mathbf{H}$, we adopt the classical ray-based channel model [1]–[4] to capture the characteristics of mmWave massive MIMO channels as

$$\mathbf{H} = \sqrt{\frac{MN}{L}} \sum_{l=1}^{L} g_l \mathbf{a}(\phi_l, N)\mathbf{a}(\theta_l, M)^H, \tag{2}$$

where L denotes the number of resolvable paths, g_l is the complex gain of the l-th path following the distribution $\mathcal{CN}(0, 1)$, ϕ_l and θ_l denotes the angle of arrival (AOA) and angle of departure (AOD) of the l-th path with $\phi_l, \theta_l \in (-\frac{\pi}{2}, \frac{\pi}{2})$, and $\mathbf{a}(\phi, M)$ is the steering vector of size $M \times 1$ with the following form,

$$\mathbf{a}(\phi, M) = \frac{1}{\sqrt{M}}\left[1, e^{j2\pi\frac{d}{\lambda}\sin\phi}, \cdots, e^{j2\pi\frac{d}{\lambda}(M-1)\sin\phi}\right], \tag{3}$$

where λ is the signal wavelength, and d is the antenna spacing, which is usually set as $d = \lambda/2$ at mmWave frequencies.

To realize CSIT acquisition at the BS, the analog precoder $\mathbf{F}_{\mathrm{RF}}$ and the digital precoder $\mathbf{F}_{\mathrm{BB}}$ are usually obtained through codebook-based channel feedback. Specifically, the user selects $\mathbf{F}_{\mathrm{RF}}$ and $\mathbf{F}_{\mathrm{BB}}$ in the analog codebook $\mathbf{C}_{\mathbf{F}_{\mathrm{RF}}}$ and digital codebook $\mathbf{C}_{\mathbf{F}_{\mathrm{BB}}}$, and then feeds back their indexes to BS. For the analog codebook of size 2^{N_A} and the digital codebook of size 2^{N_D}, the feedback overhead is N_A and N_D bits, respectively.

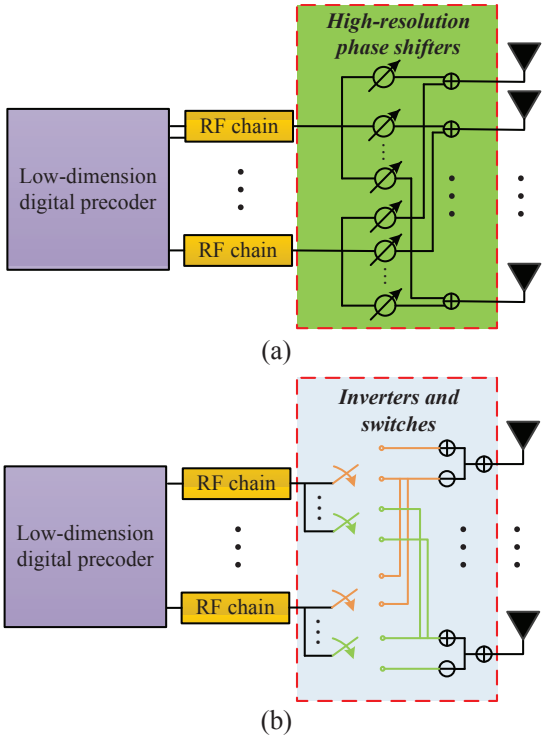

Fig. 1. Hybrid precoding for massive MIMO, where the PSs can be realized by: (a) high-resolution PSs [3]; (b) low-resolution PSs (e.g., 1-bit PSs realized by inverters and swiches [6]).

B. Low-resolution hybrid precoding

For existing hybrid precoding as shown in Fig. 1, each non-zero element of the analog precoder $\mathbf{F}_{\mathrm{RF}}$ is realized by a PS. High-resolution PSs (e.g., 7-8 bits) as shown in Fig. 1 (a) are usually used to guarantee the sum-rate performance [4]. However, the power consumption of high-resolution PSs is considerable (e.g., 40 mW for a 4-bit PS [16]). To relieve the power consumption problem, replacing high-resolution PSs (7-8 bits) with low-resolution PSs (1-2 bits) is considered to be a reasonable solution without an obvious performance loss [6]. The low-resolution PSs can be realized by switches (as shown in Fig. 1 (b), where the power consumption of one switch is only 5 mW [16]) or other power-efficient components.

For better explanation about the performance of low-resolution hybrid precoding, we analyze the array gain of low-resolution PSs as shown in **Lemma 1**.

Lemma 1. *Without loss of generality, we assume that $L = 1$ and $N = 1$. When $M \to \infty$, the ratio γ between the array gain achieved by 1-bit PSs and that by infinite-resolution PSs hybrid precoding can be presented as*

$$\lim_{M\to\infty} \gamma = \frac{4}{\pi^2}. \tag{4}$$

Proof: For the infinite-resolution PSs, the entries in the analog precoder $\mathbf{F}_{\mathrm{RF}}$ can be adjusted sufficiently close to $\mathbf{H}$. Hence, the array gain achieved by infinite-resolution PSs is $|g_1|^2$. On the contrary, the array gain achieved by 1-bit PSs can be described as

$$|\mathbf{HF}_{\mathrm{RF}}|^2 = M|g_1|^2|\mathbf{a}(\theta_1, M)^H\mathbf{F}_{\mathrm{RF}}|^2 = \frac{1}{M}|g_1|^2\left|\sum_{m=1}^{M} e^{j\beta_m}\right|^2$$

$$= \frac{1}{M}|g_1|^2\left(\left|\sum_{m=1}^{M}\cos(\beta_m)\right|^2 + \left|\sum_{m=1}^{M}\sin(\beta_m)\right|^2\right), \quad (5)$$

where elements in $\mathbf{F}_{\mathrm{RF}}$ belong to $\frac{1}{\sqrt{M}}\{-1,+1\}$ due to the constraint of 1-bit PSs, and β_m denotes the phase quantization error which can be assumed to follow the uniform distribution $\mathcal{U}(-\pi/2, \pi/2)$ for $1 \le m \le M$. Thus, we have

$$\lim_{N\to\infty}\gamma = \frac{1}{M}\left(\left|\sum_{m=1}^{M}\cos(\beta_m)\right|^2 + \left|\sum_{m=1}^{M}\sin(\beta_m)\right|^2\right),$$

$$= \mathbb{E}[\cos(\beta_m)] + \mathbb{E}[\sin(\beta_m)] = \frac{4}{\pi^2}. \quad (6)$$

The proof has been completed. ∎

Lemma 1 indicates that the performance loss caused by low-resolution PSs with low power consumption is acceptable. Thus, low-resolution PSs provide a better tradeoff between the system performance and the power consumption for hybrid precoding. However, low-resolution PSs have not been considered by existing codebooks such as the classical Grassiminien codebook [10] and the recently proposed beamsteering codebook [13]. Next, we will design an angle-based codebook for low-resolution hybrid precoding to fill in this gap.

III. Proposed Angle-Based Codebook

In this section, we firstly propose an angle-based codebook including the analog codebook and the digital codebook for low-resolution hybrid precoding. The analog codebook is composed of codewords that have array gain aligned with different AoDs. Because of the channel characteristic that path angles vary much slower than path gains, the channel feedback overhead of the proposed angle-based codebook can be significantly reduced, which will be verified by the corresponding analysis of channel feedback overhead.

A. Angle-Based Codebook

As mentioned in Section II, the channel vector $\mathbf{h}_n$ between the M-antenna BS and the n-th antenna of the user is composed of L paths, i.e., $\mathbf{h}_n$ is formed by L steering vectors' linear combination. Generally, L is much smaller than the number of BS antennas M (e.g., $L = 3$ [8]) because of the limited scattering around the BS. Therefore, the analog codebook can be designed based on the array gain of the steering vector $\mathbf{a}(\theta_l, M)$.

Without loss of generality, we omit the subscript l and consider a steering vector $\mathbf{a}(\theta, M)$ with AOD θ. Then, the array gain of $\mathbf{a}(\theta, M)$ can be calculated by

$$\boldsymbol{\eta} = \mathbf{G}^H\mathbf{a}(\theta, M), \quad (7)$$

where $\mathbf{G} = [\mathbf{a}(\alpha_1, M), \mathbf{a}(\alpha_2, M), \cdots, \mathbf{a}(\alpha_T, M)]$ with $\alpha_t = -\frac{\pi}{2} + t\frac{\pi}{T}(t = 1, 2, \cdots, T)$ and T being the grid size, and $\boldsymbol{\eta}$ of size $T \times 1$ is the array gain of $\mathbf{a}(\theta, M)$ aligned with T uniformly sampled angles in the angle domain. As α_t divides the whole angle domain uniformly into T parts, the t-th element of $\boldsymbol{\eta}$ is the array gain of $\mathbf{a}(\theta, M)$ aligned with α_t.

It is known that the optimal analog codewords are steering vectors without resolution constraint of PSs [3]. Therefore, if we design an analog codeword $\mathbf{f}_\theta$ with the array gain very close to steering vectors, the near-optimal performance under the PSs resolution constraint can be expected. Following this intuition, the analog codebook design can be formulated as,

$$\mathbf{f}_\theta = \arg\min_{\mathbf{f}\in\mathcal{F}} \|\mathbf{G}^H\mathbf{f} - \boldsymbol{\eta}\|_F, \quad (8)$$

where $\mathcal{F}$ is the set with all possible analog codewords satisfying the PSs resolution constraint.

Algorithm 1 The Neighbor Search Algorithm.

Inputs:

Antenna number M; PSs bits P; Target angle θ; Search interval D; Grid size T; Iterative number I;

Output:

Near-optimal analog codeword $\mathbf{f}_\theta$ pointing target angle θ;

1: $\mathbf{G} = [\mathbf{a}(\alpha_1, M), \cdots, \mathbf{a}(\alpha_T, M)], \alpha_t = -\pi/2 + t\frac{\pi}{T}$;
2: $\boldsymbol{\eta} = \mathbf{G}^H\mathbf{a}(\theta, M)$;
3: Randomly generate $\mathbf{f}_{\theta,(0)}$ with PSs constraint that each element belong to $\frac{1}{\sqrt{M}}\{1, e^{j\frac{1}{2^{P-1}}\pi}, \cdots, e^{j\frac{2^P-1}{2^{P-1}}\pi}\}$;
4: **for** $i = 0$; $i < I$; $i++$ **do**
5: Generate the neighbor set $\boldsymbol{\Phi}_{(i)}$ by choosing $\mathbf{f} \in \mathcal{F}$ that has D different elements from $\mathbf{f}_{\theta,(i)}$;
6: $\mathbf{f}_{\mathrm{opt},(i)} = \arg\min_{\mathbf{f}\in\boldsymbol{\Phi}_{(i)}} \|\mathbf{G}^H\mathbf{f} - \boldsymbol{\eta}\|_F$;
7: **if** $\mathbf{f}_{\theta,(i)} == \mathbf{f}_{\mathrm{opt},(i)}$ **then**
8: $\mathbf{f}_\theta = \mathbf{f}_{\theta,i}$; **break**;
9: **else**
10: $\mathbf{f}_{\theta,(i+1)} = \mathbf{f}_{\mathrm{opt},(i)}$; $\mathbf{f}_\theta = \mathbf{f}_{\mathrm{opt},(i)}$;
11: **end if**
12: **end for**
13: **return** $\mathbf{f}_\theta$.

We utilize a neighbor search algorithm (NSA) to solve (8), and the pseudo-code is shown in **Algorithm 1**. As illustrated in **Algorithm 1**, the NSA algorithm iteratively searches the neighbor set to find the codeword with the closest array gain to $\mathbf{a}(\theta, M)$. Specifically, the reference array gain of $\mathbf{a}(\theta, M)$ is constructed by $\boldsymbol{\eta} = \mathbf{G}^H\mathbf{a}(\theta, M)$ in step 2, and the initial $M \times 1$ codeword $\mathbf{f}_{\theta,(0)}$ whose elements belong to $\frac{1}{\sqrt{M}}\{1, e^{j\frac{1}{2^{P-1}}\pi}, \cdots, e^{j\frac{2^P-1}{2^{P-1}}\pi}\}$ is generated randomly in step 3. Then, for the i-th iteration, a neighbor set $\boldsymbol{\Phi}_{\theta,(i)}$ is generated by choosing all the vectors that have D different elements with $\mathbf{f}_{\theta,(i)}$ in step 5. After that, the new near-optimal codeword $\mathbf{f}_{\mathrm{opt},(i)}$ which has the array gain closer to $\mathbf{a}(\theta, M)$, is calculated by finding the best candidate in the neighbor set $\boldsymbol{\Phi}_{\theta,(i)}$ in step 6. Finally, we get the near-optimal codeword $\mathbf{f}_\theta$ which points to the target angle θ when $\mathbf{f}_{\theta,(i)}$ equals $\mathbf{f}_{\mathrm{opt},(i)}$ or number of iterations I is reached in steps 7 and 8. Due to low-resolution PSs, the number of elements in $\boldsymbol{\Phi}_{(i)}$ is small, which leads to the limited search range in each iteration.

Based on the near-optimal codeword aligned with a specific channel angle searched by the NSA, the analog codebook

can be designed to include codewords aligned with different channel angles. Specifically, the analog codebook of size $2^{N_{\rm A}}$ can be designed as $\mathbf{C}_{\mathbf{F}_{\rm RF}} = \{\mathbf{f}_1, \mathbf{f}_2, \cdots, \mathbf{f}_{2^{N_A}}\}$. Codewords $\mathbf{f}_i$ is searched by the NSA to enjoy the nearest array gain to angle $\delta_i = -\frac{\pi}{2} + (i-1)\frac{\pi}{2^{N_A}}$ for $i = 1, 2, \cdots, 2^{N_A}$. Considering these angles δ_is distribute uniformly in the angle domain, the analog codebook can uniformly cover the whole angle domain $(-\frac{\pi}{2}, \frac{\pi}{2})$ with near-optimal array gains.

For the digital precoder, we can recall that the channel matrix $\mathbf{H}$ is composed of two parts, i.e., the steering vectors decided by path angles and path gains. Considering the analog codebook $\mathbf{C}_{\mathbf{F}_{\rm RF}}$ is designed to have near-optimal array gains aligned with different AoDs, the digital codebook $\mathbf{C}_{\mathbf{F}_{\rm BB}}$ can be designed to reconstruct path gains, making the product of analog and digital precoders closer to the channel matrix $\mathbf{H}$. Since the number of RF chains $M_{\rm RF}$ is usually much smaller than the antenna number M (e.g., $M_{\rm RF} = 4, M = 64$), the digital precoder $\mathbf{F}_{\rm BB}$ is a low-dimensional matrix. To reconstruct the randomly distributed low-dimensional path gains, the classical RVQ codebook can be adapted with an acceptable quantization accuracy [11]. Hence, the digital codebook $\mathbf{C}_{\mathbf{F}_{\rm BB}}$ of size $2^{N_{\rm D}}$ can be designed as $\mathbf{C}_{\mathbf{F}_{\rm BB}} = \{\mathbf{D}_1, \mathbf{D}_2, \cdots, \mathbf{D}_{2^{N_D}}\}$, where $\mathbf{D}_i$ is an $M_{\rm RF} \times N$ matrix with all randomly distributed elements, and it satisfies the power constraint $\|\mathbf{F}_{\rm RF}\mathbf{F}_{\rm BB}\|_F^2 = \rho$.

From **Algorithm 1**, we can observe that the complexity of the NSA mainly comes from steps 2, 5 and 6. In step 2, we need to compute the array gain $\boldsymbol{\eta}$. Thus, the complexity of this part is $\mathcal{O}(M^2T)$. In step 5, the neighbor set $\mathbf{\Phi}_{\theta,(i)}$ is constructed. Since we choose $\mathbf{f} \in \mathcal{F}$ that has D different elements from $\mathbf{f}_{\theta,(i)}$, the size of $\mathbf{\Phi}_{\theta,(i)}$ is $2^P\binom{M}{D}$. In step 6, the codeword $\mathbf{f}_{\text{opt},(i)}$ is selected through $2^P\binom{M}{D}$ times calculation of the array gain. Therefore, the complexity of this part is $\mathcal{O}(2^P M^2 T\binom{M}{D})$. In summary, after I iterations, the total complexity of the NSA is $\mathcal{O}(2^P I M^2 T\binom{M}{D})$.

B. Channel Feedback Overhead Analysis

Assuming the channel matrix $\mathbf{H}$ is known at the user, which can be realized by efficient channel estimation [9], [12], the analog precoder $\mathbf{F}_{\rm RF} = [\mathbf{f}_1^{\rm RF}, \mathbf{f}_2^{\rm RF} \cdots, \mathbf{f}_{M_{\rm RF}}^{\rm RF}]$, which with $M_{\rm RF}$ analog codewords can be selected by

$$\mathbf{f}_1^{\rm RF} = \arg\max_{\mathbf{f} \in \mathbf{C}_{\mathbf{F}_{\rm RF}}} \|\mathbf{Hf}\|, \tag{9}$$

$$\mathbf{f}_i^{\rm RF} = \arg\max_{\mathbf{f} \in \mathbf{C}_{\mathbf{F}_{\rm RF}}/\{\mathbf{f}_1^{\rm RF}, \cdots, \mathbf{f}_{i-1}^{\rm RF}\}} \|\mathbf{Hf}\|, i = 2, 3, \cdots, M_{\rm RF}. \tag{10}$$

Then, the digital precoder can be chosen by maximizing the sum-rate R as

$$\mathbf{F}_{\rm BB} = \arg\max_{\mathbf{D} \in \mathbf{C}_{\mathbf{F}_{\rm BB}}} R(\mathbf{F}_{\rm RF}, \mathbf{D}), \tag{11}$$

where

$$R(\mathbf{F}_{\rm RF}, \mathbf{D}) = \log_2(|\mathbf{I}_{\rm N} + \frac{\rho}{N\sigma^2}\mathbf{H}\mathbf{F}_{\rm RF}\mathbf{D}\mathbf{D}^H{\mathbf{F}_{\rm RF}}^H\mathbf{H}^H|). \tag{12}$$

After the analog and digital codewords are picked out at the user, their indexes are fed back to the BS through the uplink channel to directly carry out hybrid precoding. Due to the selection of $M_{\rm RF}$ analog codewords, the channel feedback overhead of the proposed angle-based codebook is $M_{\rm RF}N_A$ bits for analog precoder, and N_D bits for digital precoder. However, since the surrounding scatters around the BS do not frequently change their position, the path angles mainly decided by these scatters vary much slower than the path gains [18]. Hence, the angle coherence time, during which the AoDs can be regarded as unchanged, is much larger than the classical channel coherence time. Considering that the analog codewords are designed to have array gains very close to steering vectors defined by AoDs, the analog codewords selected in (10) will keep unchanged for a much longer time than the digital codeword. Therefore, the average channel feedback overhead is close to N_D bits which is much smaller than $M_{\rm RF}N_A + N_D$.

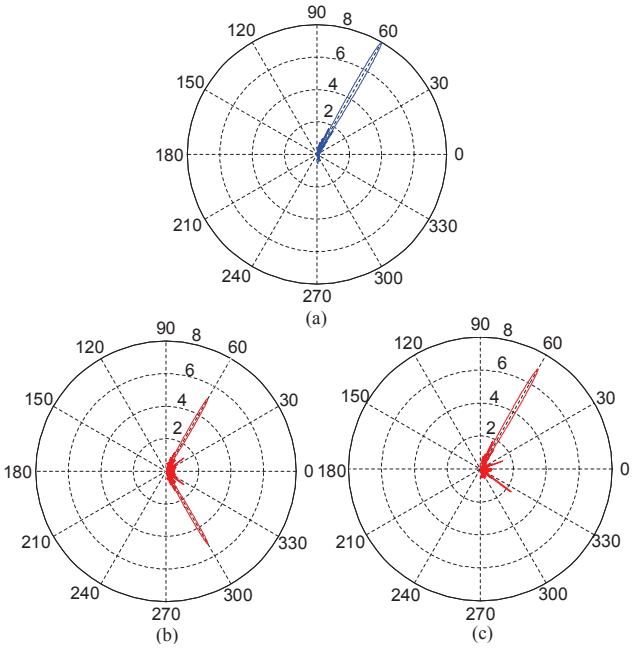

Fig. 2. Array gain comparison: (a) steering vector; (b) 1-bit codeword; (c) 2-bit codeword.

IV. Simulation Results

Simulations are carried out to verify the performance of the proposed angle-based codebook. The key simulation parameters are set as: 1) $(M, N, M_{\rm F}, L) = (64, 2, 4, 3)$; 2) The AoAs and AoDs follow the uniform distribution $\mathcal{U}(-\frac{\pi}{2}, \frac{\pi}{2})$.

Fig. 2 illustrates the array gain realized by NSA with 1-bit and 2-bit PSs compared with the benchmark. The NSA parameters are set as: target angle $\theta = \pi/3$, search interval $D = 1$, grid size $T = 1000$, iterative number $I = 100$. Fig. 2 (a) is the array gain of the ideal steering vector $\mathbf{a}(\pi/3, 64)$ which is the benchmark for comparison; Fig. 2 (b) and Fig. 2 (c) are the array gain of the codeword with 1-bit and 2-bit PSs, respectively. We can observe that the codeword obtained by NSA with 1-bit PSs has equal beam width and nearly 70% array gain compared to the ideal steering vector. Thus, the proposed angle-based codebook is able to produce narrow enough beam to distinguish different AoDs.

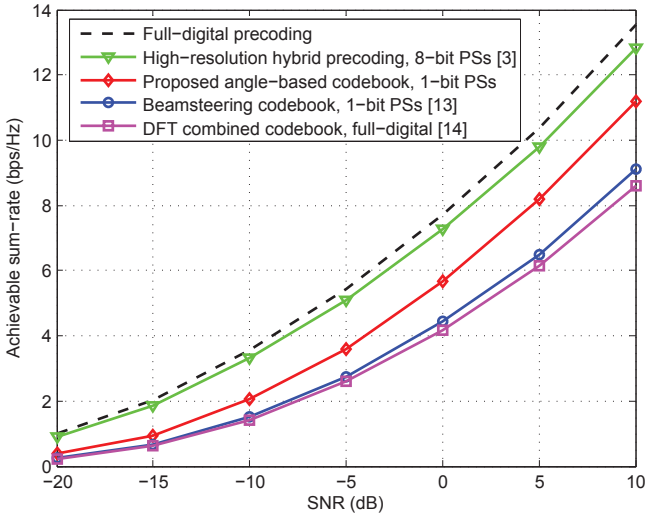

Fig. 3. Achievable sum-rate comparison for 1-bit PSs.

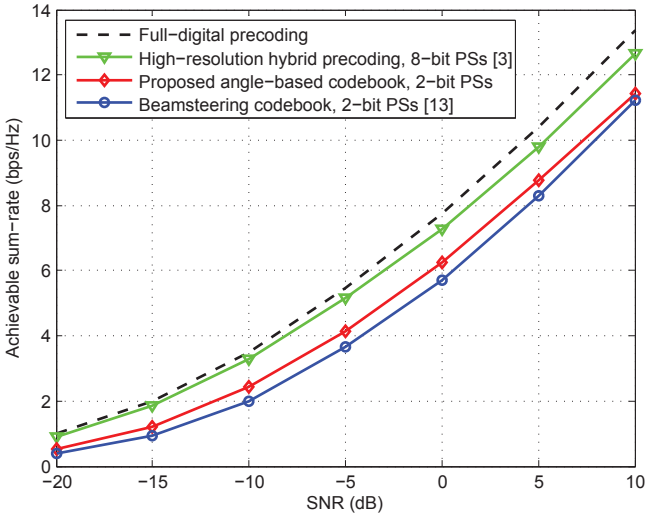

Fig. 4. Achievable sum-rate comparison for 2-bit PSs.

Fig. 3 and 4 show the achievable sum-rate performance comparison for the 1-bit and 2-bit hybrid precoding, respectively. We can observe that the angle-based codebook outperforms the DFT combined codebook [14] and beamsteering codebook [13]. Moreover, we can observe that the performance gap between angle-based codebook and ideal hybrid precoding is small, e.g. the 1-bit and 2-bit angle-based codebook can achieve 85% and 90% sum-rate performance of high-resolution hybrid precoding when SNR $= 10$.

V. Conclusions

In this paper, we have investigated the codebook design for low-resolution hybrid precoding in mmWave massive MIMO systems. We design an angle-based codebook, where the analog codebook is designed based on channel path AoDs. Under the observation that the channel vectors consists of slow-varying path AoDs and fast-varying path gains, the analog precoder selected from angle-based codebook can remain unchanged for a long time. Therefore, the channel feedback overhead can be significantly reduced. Simulation results verify that the proposed angle-based codebook is able to achieve the acceptable sum-rate performance.

Acknowledgements

This work was supported by the National Natural Science Foundation of China for Outstanding Young Scholars (Grant No. 61722109), the National Natural Science Foundation of China (Grant No. 61571270), and the Royal Academy of Engineering through the UK-China Industry Academia Partnership Programme Scheme (Grant No. UK-CIAPP\49).

References

[1] S. Mumtaz, J. Rodriquez, and L. Dai, *MmWave Massive MIMO: A Paradigm for 5G*. Academic Press, Elsevier, 2016.

[2] F. Rusek, D. Persson, B. K. Lau, E. G. Larsson, T. L. Marzetta, O. Edfors, and F. Tufvesson, "Scaling up MIMO: Opportunities and challenges with very large arrays," *IEEE Signal Process. Mag.*, vol. 30, no. 1, pp. 40–60, Jan. 2013.

[3] O. E. Ayach, S. Rajagopal, S. Abu-Surra, Z. Pi, and R. W. Heath, "Spatially sparse precoding in millimeter wave MIMO systems," *IEEE Trans. Wireless Commun.*, vol. 13, no. 3, pp. 1499–1513, Mar. 2014.

[4] R. W. Heath, N. Gonzlez-Prelcic, S. Rangan, W. Roh, and A. M. Sayeed, "An overview of signal processing techniques for millimeter wave MIMO systems," *IEEE J. Sel. Top. Signal Process.*, vol. 10, no. 3, pp. 436–453, Apr. 2016.

[5] X. Gao, L. Dai, S. Han, C. L. I, and R. W. Heath, "Energy-efficient hybrid analog and digital precoding for mmwave MIMO systems with large antenna arrays," *IEEE J. Sel. Areas Commun.*, vol. 34, no. 4, pp. 998–1009, Apr. 2016.

[6] X. Gao, L. Dai, Y. Sun, S. Han, and I. Chih-Lin, "Machine learning inspired energy-efficient hybrid precoding for mmwave massive MIMO systems," in *Proc. IEEE ICC'17*, May 2017, pp. 1–6.

[7] T. Xie, L. Dai, X. Gao, X. Dai, and Y. Zhao, "Low-complexity ssor-based precoding for massive MIMO systems," *IEEE Commun. Lett.*, vol. 20, no. 4, pp. 744–747, Apr. 2016.

[8] T. S. Rappaport, S. Sun, R. Mayzus, H. Zhao, Y. Azar, K. Wang, G. N. Wong, J. K. Schulz, M. Samimi, and F. Gutierrez, "Millimeter wave mobile communications for 5G cellular: It will work!" *IEEE Access*, vol. 1, pp. 335–349, May 2013.

[9] Z. Gao, C. Hu, L. Dai, and Z. Wang, "Channel estimation for millimeter-wave massive MIMO with hybrid precoding over frequency-selective fading channels," *IEEE Commun. Lett.*, vol. 20, no. 6, pp. 1259–1262, Jun. 2016.

[10] D. J. Love, R. W. Heath, and T. Strohmer, "Grassmannian beamforming for multiple-input multiple-output wireless systems," *IEEE Trans. Inf. Theory*, vol. 49, no. 10, pp. 2735–2747, Oct. 2003.

[11] N. Jindal, "MIMO broadcast channels with finite-rate feedback," *IEEE Trans. Inf. Theory*, vol. 52, no. 11, pp. 5045–5060, Nov. 2006.

[12] X. Rao and V. K. N. Lau, "Distributed compressive CSIT estimation and feedback for FDD multi-user massive MIMO systems," *IEEE Tran. Signal Process.*, vol. 62, no. 12, pp. 3261–3271, Jun. 2014.

[13] A. Alkhateeb, G. Leus, and R. W. Heath, "Limited feedback hybrid precoding for multi-user millimeter wave systems," *IEEE Trans. Wireless Commun.*, vol. 14, no. 11, pp. 6481–6494, Nov. 2015.

[14] J. Choi, K. Lee, D. J. Love, T. Kim, and R. W. Heath, "Advanced limited feedback designs for FD-MIMO using uniform planar arrays," in *Proc. IEEE GLOBECOM*, Dec. 2015, pp. 1–6.

[15] Z. Xiao, P. Xia, and X. G. Xia, "Codebook design for millimeter-wave channel estimation with hybrid precoding structure," *IEEE Trans. Wireless Commun.*, vol. 16, no. 1, pp. 141–153, Jan. 2017.

[16] R. Mndez-Rial, C. Rusu, N. Gonzlez-Prelcic, A. Alkhateeb, and R. W. Heath, "Hybrid MIMO architectures for millimeter wave communications: Phase shifters or switches?" *IEEE Access*, vol. 4, pp. 247–267, Jan. 2016.

[17] D. C. Arajo, E. Karipidis, A. L. F. de Almeida, and J. C. M. Mota, "Hybrid beamforming design with finite-resolution phase-shifters for frequency selective massive MIMO channels," in *Proc. IEEE ICASSP'17*, March 2017, pp. 6498–6502.

[18] V. Va, J. Choi, and R. W. Heath, "The impact of beamwidth on temporal channel variation in vehicular channels and its implications," *IEEE Trans. Veh. Technol.*, vol. 66, no. 6, pp. 5014–5029, June 2017.